On velocity/depth ambiguity in 3-D migration velocity analysis

Zhaobo Meng,* and Norman Bleistein,†
* *Center for Wave Phenomena, Colorado School of Mines; now Phillips Petroleum Company*
† *Center for Wave Phenomena, Colorado School of Mines*

ABSTRACT

In the study of analytical migration velocity analysis (AMVA), a reflector-normal velocity update procedure that imposes no dip limits was proposed. This has inspired a new way to study the velocity/depth ambiguity for post-migration velocity analysis. Here, we introduce this new study based on the analysis of the sensitivity of the reflector-normal misfit with respect to different medium parameters, particularly, velocity, depth and dip.

Moreover, based on the *least velocity/depth ambiguity* criterion, three different approaches, offset^2-AMVA (*offset-squared*-AMVA), offset-AMVA and azimuth-AMVA, are evaluated analytically. We conclude that the offset^2-AMVA is the most robust algorithm to resolve velocities and depths under large dips, and that azimuth-AMVA is the least efficient algorithm among the three. In stating that one algorithm is *more robust* than another, we mean that the *resolvability Jacobian* (introduced in this paper) is *higher order* in magnitude for this method than for the other two in an appropriate parameter used to measure robustness. This conclusion is only shown for simple background models, but we argue that this is also true for at least moderately complex models.

Introduction

Velocity/depth ambiguity in the conventional pre-migration (time domain) velocity analysis has been studied by Bickel (1990) and Lines (1993) for the horizontal reflector case. Rathor (1997) extended this analysis to the dipping reflector case. These studies answered some important questions that arose in traditional CMP time-domain velocity analysis. However, it is not clear that their conclusions apply to post-migration depth domain migration velocity analysis (MVA).

For post-migration MVA, Stork (1992b; 1992) studied velocity/depth ambiguity by applying singular value decomposition (SVD) to the linear system of the governing equations of the inverse problem. We present here an alternative approach to the analysis of this ambiguity, by characterizing the velocity/depth ambiguity analytically with respect to different MVA parameters.

The study of velocity/depth ambiguity in AMVA under different *parameters* (offset^2-AMVA, offset-AMVA and azimuth-AMVA) can be significant. We show that, the ambiguity is highly parameter dependent. Thus, the analysis of this velocity/depth ambiguity under different MVA parameters provides important information about the robustness of different AMVA approaches. Although, in general, velocity/depth ambiguity is unavoidable in MVA, we show mathematically that the "right" choice of parameter can mitigate the problem. In particular, we show that, offset^2-AMVA is superior to offset-AMVA, which, in turn, is superior to azimuth-AMVA in resolving large dips, velocities and depths. Only the offset^2-AMVA and offset-AMVA were applied in Meng *et al.* (1999a; 1999b), and azimuth-AMVA was chosen for neither of the data tests. To date, thorough comparison of the performance of offset^2-AMVA, offset-AMVA and azimuth-AMVA have not been carried out on various datasets to confirm the mathematical analysis.

AMVA in different parameters

In 2-D, offset is a popular parameter choice in MVA; often, it is the only available parameter. However, in 3-D, there is the additional choice of azimuth, when data is collected in such a manner that variable azimuth data is available. This is most easily achieved in 3-D land data. Another option that may be available is scattering angle (de Hoop & Bleistein, 1997; Brandsberg-Dahl & de Hoop, 1998). Some choice of parameter among the available options must be made. Clearly, we would want to choose a parameter for AMVA that leads to the best resolvability of the velocity and depth (possibly also under large dips).

For a medium of constant velocity with arbitrary reflecting subsurface, one can estimate the higher order partial derivatives. From Meng (1999), the second-order derivatives of the imaged point, $\mathbf{x}$, with respect to the migration velocity, c, and the MVA parameters, half-offset h and azimuth γ, along the reflector-normal direction, $\mathbf{n} = (n_1, n_2, n_3)$, (Meng, 1999; Meng *et al.*, 1999a) (Figure 1) can be obtained as

$$\frac{\partial}{\partial h}\left(n_j \frac{\partial x_j}{\partial c}\right) = \frac{1}{2}\frac{\partial}{\partial h}\left(\frac{t(\boldsymbol{\xi})}{\cos\theta}\right) = \frac{1}{2c^*}\frac{\partial}{\partial h}\left(\frac{\rho_s^* + \rho_g^*}{\cos\theta}\right) \quad (1)$$

and

$$\frac{\partial}{\partial \gamma}\left(n_j \frac{\partial x_j}{\partial c}\right) = \frac{1}{2}\frac{\partial}{\partial \gamma}\left(\frac{t(\boldsymbol{\xi})}{\cos\theta}\right) = \frac{1}{2c^*}\frac{\partial}{\partial \gamma}\left(\frac{\rho_s^* + \rho_g^*}{\cos\theta}\right), \quad (2)$$

as well as

$$\frac{\partial}{\partial c}\left(n_j \frac{\partial x_j}{\partial h}\right) = \frac{1}{2\cos\theta}\frac{\partial t(\boldsymbol{\xi})}{\partial h} = \frac{1}{2c^*\cos\theta}\frac{\partial}{\partial h}(\rho_s^* + \rho_g^*) \quad (3)$$

and

$$\frac{\partial}{\partial c}\left(n_j \frac{\partial x_j}{\partial \gamma}\right) = \frac{1}{2\cos\theta}\frac{\partial t(\boldsymbol{\xi})}{\partial \gamma} = \frac{1}{2c^*\cos\theta}\frac{\partial}{\partial \gamma}(\rho_s^* + \rho_g^*). \quad (4)$$

Here, θ is the half-opening angle, c^* is the true velocity of the model. ρ_s^* and ρ_g^* are the ray path lengths from the imaged point, $\mathbf{x}$, to the source, s, and to the receiver, g, respectively. $t(\boldsymbol{\xi})$ is the total traveltime from the imaged point to the source and the receiver. The components of the vector, $\boldsymbol{\xi} = (\xi_1, \xi_2, \gamma, h)$, are the four data acquisition parameters (Meng, 1999). If one applies AMVA with only offset data, which we call offset-AMVA, then equations (1) and (3) define a measure of the velocity/depth tradeoff in offset-AMVA. We comment that, when we refer to "depth" we mean reflector-normal depth–the image position in the reflector-normal direction (Meng, 1999). Similarly, if one applies AMVA with only azimuth data, which we call azimuth-AMVA, equations (2) and (4) define a measure of velocity/depth tradeoff in azimuth-AMVA. The smaller the magnitudes of the above second-order derivatives, the more severe the velocity/depth tradeoff will be.

To answer the question of which parameter is most robust for AMVA, we perform an asymptotic analysis. Using this approach, one can analyze these second-order derivatives more explicitly. By robust we mean an imaging algorithm whose output (the measured image) is sensitive to the model parameter (the migration velocity, c) and the measurement parameters (the half-offset, h, and/or the azimuth, γ).

We will use the quantities (Meng, 1999)

$$D(\gamma) = \frac{1}{n_3^2}(t_{13}\cos\gamma + t_{23}\sin\gamma)^2 \quad (5)$$

and

$$A(h) = \frac{n_3^2 h^2}{x_3^{*2}}, \quad (6)$$

introduced in Meng (1999). Here, $A(h)$ is assumed to be a small quantity in an asymptotic sense; that is, offset is small compared to the "projected" depth, x_3^*/n_3, where, n_3 is the cosine of the reflector dip. Also, $(t_{13},\, t_{23},\, t_{33})$ is the unit vector pointing to the zero-offset ray path, and x_3^* is the depth of the imaged point (Meng, 1999). In order to get the second-order derivatives, we need to estimate the right hand side of equation (1). We derive the results as

$$\frac{\partial}{\partial h}\left(n_j \frac{\partial x_j}{\partial c}\right)\Big|_{c=c^*} = \frac{1}{2c^*}\left(4 - \frac{1}{1+D(\gamma)}\right)A^{\frac{1}{2}}(h) + O(A^{\frac{3}{2}}(h)) \quad (7)$$

and

$$\frac{\partial}{\partial \gamma}\left(n_j \frac{\partial x_j}{\partial c}\right)\Big|_{c=c^*} = \frac{x_3^* D'(\gamma) A(h)}{4c^* n_3 (1+D(\gamma))^2} + O(A^2(h)). \quad (8)$$

Similarly,

$$n_j \frac{\partial^2 x_j}{\partial c \partial h}\Big|_{c=c^*} = \frac{1}{c^*}\left(2 - \frac{1}{1+D(\gamma)}\right)A^{\frac{1}{2}}(h) + O(A^{\frac{3}{2}}(h)) \quad (9)$$

and

$$n_j \frac{\partial^2 x_j}{\partial c \partial \gamma}\Big|_{c=c^*} = \frac{x_3^* D'(\gamma) A(h)}{2c^* n_3 (1+D(\gamma))^2} + O(A^2(h)). \quad (10)$$

Thus, we also obtain the following mixed second-order derivatives

$$\frac{\partial n_j}{\partial h}\frac{\partial x_j}{\partial c}\Big|_{c=c^*} = \frac{A^{\frac{1}{2}}(h)}{2c^*(1+D(\gamma))} + O(A^{\frac{3}{2}}(h)) \quad (11)$$

and

$$\frac{\partial n_j}{\partial \gamma}\frac{\partial x_j}{\partial c}\Big|_{c=c^*} = -\frac{x_3^* D'(\gamma) A(h)}{4c^* n_3 (1+D(\gamma))} + O(A^2(h)). \quad (12)$$

It is interesting to note that, from equation (1), the second-order derivative with respect to h^2 ($\sim A(h)$), is obtained as

$$\frac{\partial}{\partial (h^2)}\left(n_j \frac{\partial x_j}{\partial c}\right)\Big|_{c=c^*} = \frac{n_3}{4c^* x_3^*}\left(4 - \frac{1}{1+D(\gamma)}\right) + O(A(h)). \quad (13)$$

Thus, we conclude that

$$n_j \frac{\partial^2 x_j}{\partial (h^2) \partial c}\Big|_{c=c^*} = \frac{n_j}{2h}\frac{\partial^2 x_j}{\partial h \partial c}\Big|_{c=c^*} = O(1), \quad (14)$$

$$n_j \frac{\partial^2 x_j}{\partial h \partial c}\Big|_{c=c^*} = O(A^{\frac{1}{2}}(h)), \quad (15)$$

and

$$n_j \frac{\partial^2 x_j}{\partial\gamma\partial c}\,|_{c=c^*} = O(A(h)). \qquad (16)$$

Comparison of the leading terms of the above second-order derivatives leads to the important conclusion that $n_j \partial^2 x_j/\partial(h^2)\partial c$ is two orders of magnitude higher in $\sqrt{A(h)}$ than $n_j\partial^2 x_j/\partial\gamma\partial c$. Similarly, $n_j\partial^2 x_j/\partial h\partial c$ is one order higher of magnitude than this last expression in $\sqrt{A(h)}$.

For the case of small offset compared to depth and for constant background models with arbitrary reflecting subsurface, the results derived above indicate that, an offset^2-AMVA is superior to offset-AMVA, and offset-AMVA is superior to azimuth-AMVA. We summarize the following:

- The larger the reflector dip, the smaller the n_3, and the worse the velocity/depth ambiguity.
- For the same dip, offset^2-AMVA is superior to offset-AMVA, and offset-AMVA is superior to azimuth-AMVA.

Azimuth-AMVA has inferior performance in our analysis, so we will study only offset^2-AMVA and offset-AMVA in the next section.

There is a similarity between the prestack time domain NMO and post-migration depth domain reflector-normal misfit. As is well known, normal moveout in prestack time domain is a function of offset^2. So is the reflector-normal misfit in post-migration depth domain, since one can freely switch the source and receiver without changing the misfit. For simple background models, the normal moveout is quadratic in offset and linear in offset^2 (Yilmaz, 1987); and so is the reflector-normal misfit (Meng, 1999). This simply indicates that, for simple background models, reflector-normal misfit bears a better linearity with respect to offset^2 than to offset. This explains why offset^2-AMVA is superior to offset-AMVA, at least for background models with modest complexity.

Further analysis for offset^2-AMVA and offset-AMVA

We have analyzed offset^2-AMVA, offset-AMVA and azimuth-AMVA for constant background models with arbitrary reflecting subsurface. We now further simplify the background models to models with flat reflectors for a more explicit analysis of offset^2-AMVA and offset-AMVA.

For models with a constant background and horizontal reflecting subsurface, the measured quantities do not depend on the azimuth. Therefore, the azimuth variable, γ, is omitted in the following expressions. In addition, in this case, the reflector-normal misfits are equivalent to the depth misfits. Now, suppose, after a

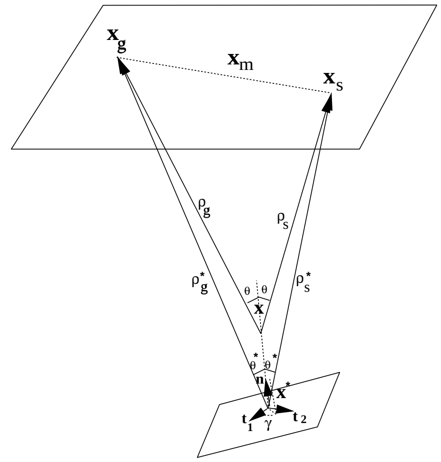

Figure 1. Ray patterns for AMVA in a constant velocity background media. $\mathbf{x}^*(c^*)$ is the true reflector position. $\rho_s^*(c^*)$ and $\rho_g^*(c^*)$ are the ray paths corresponding to the true velocity, c^*. Thus, $\rho_s^*(c^*)$ and $\rho_g^*(c^*)$ do not depend on γ and h. $\rho_s(\gamma, h; c, c^*)$ and $\rho_g(\gamma, h; c, c^*)$ are the ray paths, and $\mathbf{x}(\gamma, h; c, c^*)$ is the imaged point by using data with azimuth, γ, and half-offset, h, migrated with erroneous velocity, c. Here, axes $\mathbf{t}_1, \mathbf{t}_2, \mathbf{n}$ form the local orthogonal coordinates.

horizon-based prestack depth migration (HPSDM) (Wyatt, 1995), there is a reflector at depth $x_3(h; c, c^*)$. Since this reflector is obtained by migrating the data with a constant migration velocity, c, the migrated image of the reflector can be explicitly written as a function of the half-offset, h, as

$$x_3(h; c, c^*) = (c^2 t^2(h; c^*)/4 - h^2)^{\frac{1}{2}}. \qquad (17)$$

The true model is assumed to be a constant model with velocity, c^*, and the true traveltime is given by

$$t(h; c^*) = \frac{2}{c^*}(h^2 + x_3^{*2})^{\frac{1}{2}}, \qquad (18)$$

where x_3^* is the true depth of the reflector. Substituting $t(h; c^*)$ of equation (18) into equation (17) yields

$$x_3^2(h; c, c^*) + h^2 = \frac{c^2}{c^{*2}}(x_3^{*2} + h^2). \qquad (19)$$

The above equation describes the relationship between the migrated depth, $x_3(h; c, c^*)$, and the true depth of the reflector, x_3^*, due to the use of wrong velocity $c \neq c^*$.

From equation (19), we can write the depth of the migration image associated with the reflector, $x_3(h; c, c^*)$ as a function of the migration velocity, c, and the offset, h, as

$$x_3(h; c, c^*) = \sqrt{\frac{c^2}{c^{*2}}(x_3^{*2} + h^2) - h^2}. \qquad (20)$$

The reflector-normal misfits (depth misfits) are defined by

$$L(h; c, c^*) \equiv x_3(h; c, c^*) - x_3^*, \qquad (21)$$

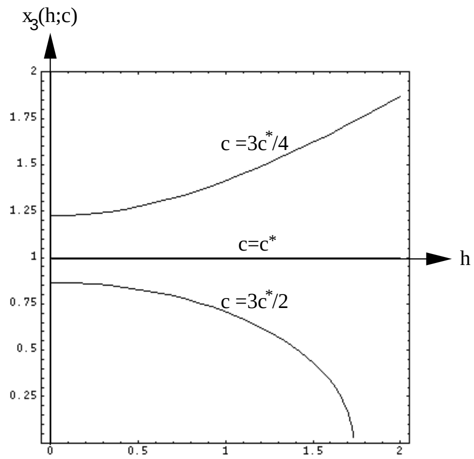

Figure 2. Migration depth versus half-offset, h, in a model with a horizontal reflector and constant velocity. Depth migration with different migration velocities are compared, such as $c^2 = 3c^{*2}/4$ (upper, "smile", over-estimated), $c = c^*$ (horizontal, exact) and $c^2 = 3c^{*2}/2$ (lower, "frown", under-estimated), respectively.

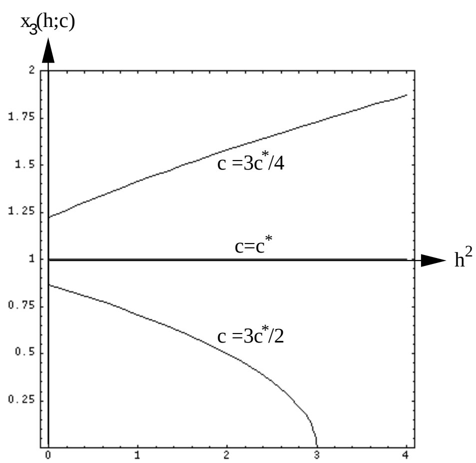

Figure 3. Migration depth versus half-offset squared, h^2, in a model with a horizontal reflector and constant velocity. Depth migration with different velocities are compared, such as $c^2 = 3c^{*2}/4$ (upper, "smile", over-estimated), $c = c^*$ (horizontal, exact) and $c^2 = 3c^{*2}/2$ (lower, "frown", under-estimated), respectively.

and are functions of the migration depth and the true depth as a function of migration velocity, c, and the half-offset, h. Figure 2 shows the reflector-normal misfit versus half-offset, h, in a model with a horizontal reflector and constant velocity, for different migration velocities. Figure 3 shows the reflector-normal misfit versus half-offset squared, h^2, in a model with a horizontal reflector and constant velocity, for the three different migration velocities. To further analyze the migration depth, we differentiate equation (20) with respect to half-offset, h,

$$\frac{\partial x_3(h;c,c^*)}{\partial h} = \frac{(c^2/c^{*2}-1)h}{x_3(h;c,c^*)}; \tag{22}$$

and we differentiate equation (20) with respect to half-offset, h^2,

$$\frac{\partial x_3(h;c,c^*)}{\partial (h^2)} = \frac{c^2/c^{*2}-1}{2x_3(h;c,c^*)}. \tag{23}$$

Similarly, differentiating equation (20) with respect to migration velocity, c, yields

$$\frac{\partial x_3(h;c,c^*)}{\partial c} = \frac{c(x_3^{*2}+h^2)}{c^{*2}x_3(h;c,c^*)}. \tag{24}$$

To obtain the second-order partial derivative, we differentiate equation (24) with respect to half-offset h again, yielding

$$\frac{\partial^2 x_3(h;c,c^*)}{\partial c \partial h} \,|_{c=c^*} = \frac{2h}{c^* x_3^*} > 0. \tag{25}$$

Following Meng (1999), differentiating equation (24) with respect to the half-offset squared, h^2, yields

$$\frac{\partial^2 x_3(h;c,c^*)}{\partial c \partial (h^2)} \,|_{c=c^*} = \frac{1}{c^* x_3^*} > 0. \tag{26}$$

Following Liu (1995) and Liu & Bleistein (1995), the relationship (25) shows us that *"accuracy of velocity analysis for a CIG derived from common-offset images is better when the two offsets are large and differ from one another, and the targets are shallow"* (Liu & Bleistein, 1995). Moreover, the accuracy of velocity analysis is better when the true velocity is low than when it is high. This last is well-known but not previously quantified, as we have, here.

Recall that the goal of AMVA in this section is to find the true depth, x_3^*, and the true velocity, c^*, from the migration depth, $x_3(h;c,c^*)$. The migration depth, $x_3(h;c,c^*)$, is provided for a certain half-offset, h, and migration velocity, c, in the 2-D h-c measurement panel. Thus, the following Jacobian matrix (the *offset-resolvability Jacobian*) measures how well such a 2-D inverse problem for c^* and x_3^* can be determined by using measurements in h and c, for c being nearly equal to c^*:

$$\mathcal{J}^h \,|_{c=c^*} = \begin{vmatrix} \frac{\partial^2 x_3(h;c,c^*)}{\partial h^2} & \frac{\partial^2 x_3(h;c,c^*)}{\partial h \partial c} \\ \frac{\partial^2 x_3(h;c,c^*)}{\partial h \partial c} & \frac{\partial^2 x_3(h;c,c^*)}{\partial c^2} \end{vmatrix}_{c=c^*}$$

$$= -\left(\frac{\partial^2 x_3(h;c,c^*)}{\partial h \partial c}\right)^2 |_{c=c^*} = -\frac{4h^2}{c^{*2}x_3^{*2}}. \tag{27}$$

Similarly, the following Jacobian matrix (*the offset*^{2}*-resolvability Jacobian*) measures how well such a 2-D inverse problem for c^* and x_3^* can be determined by using measurements in h^2 and c, for c being nearly equal to c^*:

$$\mathcal{J}^{h^2}\mid_{c=c^*}= \begin{vmatrix} \frac{\partial^2 x_3(h;c,c^*)}{\partial (h^2)^2} & \frac{\partial^2 x_3(h;c,c^*)}{\partial (h^2)\partial c} \\ \frac{\partial^2 x_3(h;c,c^*)}{\partial (h^2)\partial c} & \frac{\partial^2 x_3(h;c,c^*)}{\partial c^2} \end{vmatrix}_{c=c^*} . \quad (28)$$

Since

$$\frac{\partial^2 x_3(h;c,c^*)}{\partial h^2}\mid_{c=c^*}=0 \quad (29)$$

and

$$\frac{\partial^2 x_3(h;c,c^*)}{\partial (h^2)^2}\mid_{c=c^*}=0, \quad (30)$$

it follows that

$$\mathcal{J}^{h^2}\mid_{c=c^*}=-\left(\frac{\partial^2 x_3(h;c,c^*)}{\partial (h^2)\partial c}\right)^2\mid_{c=c^*}=-\frac{1}{c^{*2}x_3^{*2}}. \quad (31)$$

For offset-AMVA, the offset-resolvability Jacobian (27) indicates that there exists a unique solution if and only if $\mathcal{J}^h$, defined in equation (27), does not vanish. Thus, equation (27) gives a measure to the velocity/depth tradeoff for offset-AMVA. From equation (27), the velocity/depth tradeoff can be interpreted as *the lack of variations of the partial derivative,* $\partial x_3(h;c,c^*)/\partial c \mid_{c=c^*}$*, with respect to the half-offset,* h. From the above expression, we conclude that, for offset-AMVA:

- The larger the half-offset, h, the smaller the velocity/depth tradeoff.
- The deeper the imaged point is, the larger the velocity/depth tradeoff.
- The higher the true velocity is, the larger the velocity/depth tradeoff.

For offset^2-AMVA, the offset^2-resolvability Jacobian (27) indicates that there exists a unique solution if and only if $\mathcal{J}^{h^2}$, does not vanish. Thus, equation (27) gives a measure to the velocity/depth tradeoff for offset^2-AMVA. From equation (27), the velocity/depth tradeoff can be interpreted as *the lack of variations of the partial derivative,* $\partial x_3(h;c,c^*)/\partial c \mid_{c=c^*}$*, with respect to the half-offset squared,* h^2. From the above expression, we conclude that, for offset^2-AMVA:

- Offset does not have to be small.
- The deeper the imaged point is, the larger the velocity/depth tradeoff.
- The higher the true velocity is, the larger the velocity/depth tradeoff.

To more strictly verify the above conclusions, an analysis in dimensionless variables is included in the Appendix to this paper.

Conclusions

In the study of reflector-normal velocity update (Meng *et al.*, 1999a; Meng *et al.*, 1999b), we have developed a new way to analyze the velocity/depth ambiguity for post-migration AMVA.

This analysis is carried out by analyzing the reflector-normal misfit with respect to different AMVA parameters, particularly, offset^2, offset and azimuth. The study reveals how an AMVA algorithm resolves velocity, and depth under large dips. We conclude that, with velocity/depth ambiguity as a criterion, offset^2-AMVA is superior to offset-AMVA, and is further superior (the resolvability Jacobian is orders higher) to azimuth-AMVA. In fact, offset^2-AMVA has demonstrated *outstanding* sensitivity to the migration and model parameters, such as the reflector dip, migration velocity and image depth, over offset-AMVA and azimuth-AMVA.

The offset^2-AMVA and offset-AMVA algorithms were tested in Meng *et al.* (1999a; 1999b). However, a thorough comparison of the three approaches on various 3-D synthetic and field data has not yet been tested to further verify our theory.

Acknowledgments

We are thankful for the numerous stimulating discussions with Kay D. Wyatt, Paul A. Valasek and Bob Heaton of Phillips Petroleum Company. We are also grateful to Phillips Petroleum Company, who has provided all support for this research work, both on-site and off-site. The authors appreciate the insightful discussions with Zhenyue Liu at CWP/CSM (now at Exxon), Jennifer Swanson, Jerry W. Brown, Yunqing Shen, Brian K. Macy and Wei Liu from Phillips. The first author greatly acknowledges the financial support by Phillips and the Office of Naval Research, through CWP, as well as the partial support by the sponsors of the Consortium Project on Seismic Inverse Methods for Complex Structures at the Center for Wave Phenomena, Colorado School of Mines.

References

Al-Yahya, K. 1989. Velocity analysis by iterative profile migration. *Geophysics*, **54**, 718–729.

Bickel, S. H. 1990. Velocity-depth ambiguity of reflection traveltimes. *Geophysics*, **55**, 266–276.

Brandsberg-Dahl, S., & de Hoop, M. V. 1998. Common scattering angle sections. *Pages 1–8 of: Center for Wave Phenomena Annual Report, CWP-267.*

de Hoop, M. V., & Bleistein, N. 1997. Generalized Radon transform inversion for refelctivity in anisotropic elastic media. *Inverse Problems*, **13**, 669–690.
Deregowski, S. M. 1990. Common-offset migrations and velocity analysis. *First Break*, **8**, 225–234.
Lines, L. 1993. Ambiguity in analysis of velocity and depth. *Geophysics*, **58**, 596–597.
Liu, Z. 1995. Migration velocity analysis. *Pages 1–88 of: Ph. D. thesis, Colorado School of Mines.*
Liu, Z., & Bleistein, N. 1995. Migration velocity analysis: Theory and an iterative algorithm. *Geophysics*, **60**, 142–153.
MacKay, S., & Abma, R. 1992. Imaging and velocity estimation with depth-focusing analysis. *Geophysics*, **57**(12), 1608–1622.
Meng, Z. 1999. Tetrahedral Based Earth Models, Ray Tracing in Tetrahedral Models and Analytical Migration Velocity Analysis. *Pages 1–180 of: Ph. D. thesis, Colorado School of Mines, CWP-296.*
Meng, Z., Bleistein, N., & Wyatt, K. D. 1999a. 3-D Analytical Migration Velocity Analysis I: Two-step Velocity Estimation by Reflector-normal Update. *This report.*
Meng, Z., Bleistein, N., & Valasek, P. A. 1999b. 3-D Analytical Migration Velocity Analysis II: Velocity Gradient Estimation. *This report.*
Rathor, B. S. 1997. Velocity-depth ambiguity in the dipping reflector case. *Geophysics*, **62**, 1583–1585.
Stork, C. 1992a. Reflection tomography in the postmigrated domain. *Geophysics*, **57**, 680–592.
Stork, C. 1992b. Singular value decomposition of the velocity-refelctor depth tradeoff, part 2: Hign resolution analysis of a generic model. *Geophysics*, **57**, 933–943.
Stork, C., & Clayton, R. W. 1992. Using constraints to address the instabilities of automated prestack velocity analysis. *Geophysics*, **57**, 404–419.
Wyatt, K. D. et. al. 1995. Rapid velocity estimation using horizon-based 3-D prestack depth migration. *In: Research workshop: "Velocity Estimation for 3-D Imaging", 65th Annual Internat. Mtg., Soc. Expl. Geophys*, vol. 65.
Yilmaz, O. 1987. *Seismic data processing.* Tulsa: Society of Exploration Geophysics.

APPENDIX A: Analysis of the reflector-normal misfit

The zero-offset/azimuth imaging conditions were derived in Meng *et al.* (1999a). To apply AMVA, one must estimate the imaged point, $\mathbf{x} = (x_1, x_2, x_3)$, as a function of the migration parameters. Mathematically, we need the complete differences of the imaged point, $\mathbf{x}$, with respect to the MVA parameters. In this paper, we limit our discussion to these MVA parameters: half-offset, h, (also, h^2) and azimuth, γ. In practice, when the partial derivatives $\partial x_j/\partial\gamma$ and $\partial x_j/\partial h$ are applied to common image gather (CIG) data, it is important to note that the position of the *midpoint* varies with h and γ; that is, the derivative of the imaged point $\mathbf{x}$, with respect to the half-offset, h, or the azimuth, γ, may contain extra terms related to the midpoint $(\xi_1, \xi_2, 0)$ (Figure A1). The question arises as to how important these variations are in AMVA. This is because, the midpoint may vary with γ and h (i.e., $\partial\xi_i/\partial\gamma \neq 0$ or $\partial\xi_i/\partial h \neq 0$, for $i = 1$ or 2) as well. This can be stated more precisely as

$$\frac{d\mathbf{x}}{d\gamma} = \frac{\partial\mathbf{x}}{\partial\gamma} + \frac{\partial\mathbf{x}}{\partial\xi_1}\frac{\partial\xi_1}{\partial\gamma} + \frac{\partial\mathbf{x}}{\partial\xi_2}\frac{\partial\xi_2}{\partial\gamma} \tag{A1}$$

and

$$\frac{d\mathbf{x}}{dh} = \frac{\partial\mathbf{x}}{\partial h} + \frac{\partial\mathbf{x}}{\partial\xi_1}\frac{\partial\xi_1}{\partial h} + \frac{\partial\mathbf{x}}{\partial\xi_2}\frac{\partial\xi_2}{\partial h}. \tag{A2}$$

Thus, the issue is whether or not the last two terms in equations (A1) and (A2) can be neglected. This is standardly done in traditional post-migration velocity analysis approaches (Al-Yahya, 1989; Deregowski, 1990; MacKay & Abma, 1992; Stork, 1992a; Wyatt, 1995). It was shown in Appendix C.1 in Meng (1999) that these last two terms in equations (A1) and (A2) are, for a constant background model with an arbitrarily varying reflecting subsurface, indeed, orders of magnitude smaller than the first term. We argue "by continuity" that this conclusion holds for models with small variations in the background as well. Thus, this verifies that MVA can be carried out in h and γ, while neglecting the last two terms in (A1) and (A2).

APPENDIX B: Analysis of the Jacobians in Dimensionless Variables

Each Jacobian defined in equations (27) and (31) gives a measure of the "well-conditionedness" of the inverse problem in terms of the migration parameters, c and h or h^2. However, these Jacobians are defined in different dimensions. Hence, in the following, we introduce the dimensionless counterparts of the above quantities. First, the dimensionless relative imaged depth, χ, is defined, as

$$\chi = x_3/x_3^*. \tag{B1}$$

Second, the dimensionless relative velocity, ν, is defined, as

$$\nu = c/c^*. \tag{B2}$$

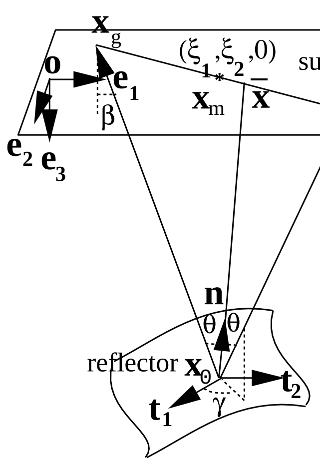

Figure A1. The reflection pattern $\mathbf{x}_0$ is the reflector $\mathbf{t}_1$ and $\mathbf{t}_2$ are the two orthonormal tangential vectors and $\mathbf{n}$ is the normal to the reflector. γ is the azimuth with respect to axis $\mathbf{t}_1$ and θ^* is the half-opening angle of the two ray vectors. $\mathbf{x}_s$ and $\mathbf{x}_g$ are the source and geophone positions, respectively. $\mathbf{x}_m$ is the midpoint. $\mathbf{e}_3$ is the normal to the datum surface. In the figure, $\mathbf{e}_1$, $\mathbf{e}_2$ and $\mathbf{e}_3$ form the global coordinate system, and $(\xi_1, \xi_2, 0)$ is the midpoint.

Finally, the dimensionless relative offset, η, is defined as *

$$\eta = h/x_3^*. \tag{B3}$$

With the above new dimensionless migration parameters, ν and η, equation (20) is equivalent to

$$\chi(\nu,\eta) = \sqrt{\nu^2(1+\eta^2) - \eta^2}, \tag{B4}$$

and, its first order partial derivatives with respect to η and η^2 are given by

$$\frac{\partial\chi}{\partial\eta} = \frac{\eta(\nu^2-1)}{\chi(\nu,\eta)} \tag{B5}$$

and

$$\frac{\partial\chi}{\partial(\eta^2)} = \frac{\nu^2-1}{2\chi(\nu,\eta)}, \tag{B6}$$

respectively. Furthermore, its second order mixed partial derivatives with respect to η, ν and η, ν^2 (at $\nu = 1$ or $c = c^*$) are given by

$$\frac{\partial^2\chi}{\partial\eta\partial\nu} \mid_{\nu=1} = \frac{2\nu\eta}{\chi^2(\nu,\eta)} \mid_{\nu=1} = 2\eta \tag{B7}$$

and

$$\frac{\partial^2\chi}{\partial(\eta^2)\partial\nu} \mid_{\nu=1} = \frac{\nu}{\chi^2(\nu,\eta)} \mid_{\nu=1} = 1, \tag{B8}$$

respectively.

Now, we obtain the dimensionless offset^2-resolvability Jacobian and the dimensionless offset-resolvability Jacobian (at $\nu = 1$ or equivalently, $c = c^*$ as in the previous discussion), with respect to the dimensionless migration parameters, ν, η and ν, η^2, as

$$\mathcal{J}^\eta \mid_{\nu=1} = \begin{vmatrix} \dfrac{\partial^2\chi(\nu,\eta)}{\partial\eta^2} & \dfrac{\partial^2\chi(\nu,\eta)}{\partial\eta\partial\nu} \\ \dfrac{\partial^2\chi(\nu,\eta)}{\partial\eta\partial\nu} & \dfrac{\partial^2\chi(\nu,\eta)}{\partial\nu^2} \end{vmatrix}_{\nu=1}$$

$$= -\left(\frac{\partial^2\chi(\nu,\eta)}{\partial\eta\partial\nu}\right)^2 \mid_{\nu=1} = -4\eta^2 \tag{B9}$$

and

$$\mathcal{J}^{\eta^2} \mid_{\nu=1} = \begin{vmatrix} \dfrac{\partial^2\chi(\nu,\eta)}{\partial(\eta^2)^2} & \dfrac{\partial^2\chi(\nu,\eta)}{\partial(\eta^2)\partial\nu} \\ \dfrac{\partial^2\chi(\nu,\eta)}{\partial(\eta^2)\partial\nu} & \dfrac{\partial^2\chi(\nu,\eta)}{\partial\nu^2} \end{vmatrix}_{\nu=1}$$

$$= -\left(\frac{\partial^2\chi(\nu,\eta)}{\partial(\eta)^2\partial\nu}\right)^2 \mid_{\nu=1} = -1, \tag{B10}$$

respectively.

The above analysis shows that the Jacobian with respect to η and ν is $O(\eta^2)$, while the Jacobian with respect to η^2 and ν is $O(1)$. The former is two orders lower in magnitude in η than the latter. This indicates that offset^2-AMVA (or η^2-AMVA) is superior to offset-AMVA (or η-AMVA), as far as AMVA is considered an inverse problem. Again, this conclusion applies to constant background models with flat subsurface reflectors. However, we argue that this is true for models with at least mildly varying background as well.

* One of the dimensionless migration parameters, η, is regarded as the small quantity in the perturbation analysis. In equation (6), a small quantity, A, for more general background media, is introduced. For constant background model with a flat reflector as in this section, $\eta = \sqrt{A}$.